Article ID: 1006-8775(2017) 03-0269-12

NUMERICAL SIMULATION STUDY ON THE RAPID INTENSIFICATION OF TYPHOON HAIKUI (1211) OFF THE SHORE OF CHINA

ZHANG Sheng-jun (张胜军)[1], QIAN Yan-zhen (钱燕珍)[2], HUANG Yi-wu (黄奕武)[3]
GUO Jian-min (郭建民)[2]
(1. State Key Laboratory of Severe Weather, Chinese Academy of Meteorological Sciences, Beijing 100081 China;
2. Ningbo Meteorological Observatory, Ningbo 315012 China;
3. National Meteorological Center, Beijing 100081 China)

Abstract: Forecasting the rapid intensification of tropical cyclones over offshore areas remains difficult. In this article, the Weather Research and Forecast (WRF) model was used to study the rapid intensification of Typhoon Haikui (1211) off the shore of China. After successful simulation of the intensity change and track of the typhoon, the model output was further analyzed to determine the mechanism of the rapid change in intensity. The results indicated that a remarkable increase in low-level moisture transportation toward the inner core, favorable large-scale background field with low-level convergence, and high-level divergence played key roles in the rapid intensification of Typhoon Haikui in which high-level divergence could be used as an indicator for the rapid intensity change of Typhoon Haikui approximately 6 h in advance. An analysis of the typhoon structure revealed that Typhoon Haikui was structurally symmetric during the rapid intensification and the range of the eyewall was small in the low level but extended outward in the high level. In addition, the vertically ascending motion, the radial and tangential along wind speeds increased with increasing typhoon intensity, especially during the process of rapid intensification. Furthermore, the intensity of the warm core of the typhoon increased during the intensification process with the warm core extending outward and toward the lower layer. All of the above structural changes contributed to the maintenance and development of typhoon intensity.

Key words: typhoon; rapid change of typhoon intensity; structure change; numerical simulation
CLC number: P444 **Document code:** A
doi: 10.16555/j.1006-8775.2017.03.004

1 INTRODUCTION

Most global tropical cyclones (TCs) are generated in the Northwest Pacific, and China is one of the countries that are most severely affected by TCs. The change in intensity and structure of a TC are related to the magnitude of the TC disaster. Chen et al.[1] introduced the concepts of "slowly changing" and "rapidly changing" in 1979. Yan[2] analyzed the intensity distribution of TCs in the Northwest Pacific and proposed the following criterion for the rapid intensification of an offshore TC in China: the absolute value of the change in maximum wind speed near the center of the TC is ⩾10 m/s with 12 h. Yu et al.[3] measured TC intensity using the minimum sea surface pressure in the center of the TC and proposed a criterion for sudden increases in TC intensity. Yu et al.[4] suggested that TC intensity gradually shifts from increasing to attenuating owing to the influence of the continental shelf when the TC is near land. The number of the intensified TCs before landfall accounted for merely 13% of the samples, and 80% of TCs landing in China were weakened within 36 h before landfall. The data of Zhu et al.[5] indicated that 12.58% of TCs were rapidly intensified when moving to the offshore of China. Though the case of rapid typhoon intensification offshore area is rare, but with obvious disaster, this phenomenon of the rapid intensification of typhoon intensity is a difficulty and emphases in the typhoon operational forecasting[6].

Our ability to predict TC structure and intensity change lags behind our capability to predict TC track[7] owing to the absence of sufficient sea observation data, low model resolution, and an inadequate understanding of the physical processes involved in TC intensity change. Chen et al.[8] reviewed studies on TCs in the last century and pointed out that changes in TC intensity could be correlated with cold air intensity, high-altitude torrent, westerly wind deep trough, mesoscale and microscale systems, topographical role, sea surface temperature, and spray. Duan et al.[9] reviewed more recent studies on TC intensity and considered factors

Received 2016-01-29; **Revised** 2017-07-17; **Accepted** 2017-08-15
Foundation item: National Key Basic Research Program of China (2015CB452804); National Natural Science Foundation of China (41575063, 41275066, 41075037); Ningbo Science and Technology Project (2014C50024)
Biography: ZHANG Sheng-jun, Ph. D., Associate Research Fellow, primarily undertaking research on mesoscale meteorology and numerical simulations.
Corresponding author: QIAN Yan-zhen, e-mail: qian-y-z@163.com

including TC occurrence, maximum possible intensity, and environmental effects. Some studies have investigated the effects of large-scale environmental conditions on TC intensity change [10-13]; the results suggest that the interaction between the tropospheric conditions and the TC outflow play a critical role in the intensity change of TC off the shore of China. Lei et al.[14] qualitatively analyzed the influence of large-scale environmental fields by building equations for change in TC intensity. Studies on changes in typhoon structure and intensity have focused on the relationships between changes in typhoon intensity and different aspects including mesoscale dynamic processes inside the typhoon, vortex Rossby waves, and baroclinic characteristics. Wang[15] further suggested that the vertical wind shear not only affected the TC intensity, but also the TC structure (e.g., the cloud wall of the typhoon eye and the spiral rain band). Other studies indicated that non-axisymmetric perturbations superimposed on the typhoon circulation are typically absorbed by basic flow[16-17]; however, these perturbations can develop, spread, and affect the typhoon intensity under some conditions. Therefore, a typhoon may maintain or intensify by gaining vorticity from the mesoscale convective systems involved into typhoon circulation[18-19]. The mechanisms of the rapid increase in the intensity of Typhoon Saomai (2006) were studied using numerical simulations[20-21]. The above shows that most of the past studies on the rapid intensification of typhoon intensity focused on the diagnostic analyses of large-scale background fields and numerical experiments of idealized fields, and numerical simulations on real typhoons were rare. Thus, it is essential to conduct more studies on rapid intensification in real typhoons to elucidate the associated mechanisms. Such studies will help improve the operational forecasting of typhoon intensity.

Typhoon Haikui (1211) occurred in the Northwest Pacific at 08:00 on August 3, 2012 (Unless otherwise specified, the time involved in the analysis is Beijing Time). Haikui intensified to a tropical storm at 17:00 on August 5 and further intensified to a typhoon at 17:00 on August 6. Typhoon Haikui landed in Hepu Town, Xiangshan County, Zhejian at 03:20 on August 8 and was weakened in Anhui at 14:00 on August 9. According to the intensity determined by China Meteorological Administration (CMA), the maximum wind speed near the typhoon center increased from 35 to 48 ms^{-1} from 11:00 to 17:00 on August 7, an increase of 13 ms^{-1} in a short 6-h period. During this period, the central pressure decreased from 965 to 945 hPa. Hence, the intensity change of Typhoon Haikui was characterized in offshore rapid intensification of typhoon intensity. Joint Typhoon Warning Center (JTWC) and Regional Specialized Meteorology Center (RSMC) Tokyo-Typhoon Center did not reflect this drastic intensification process and reported the maximum wind speed as 33 ms^{-1}. The author has verified the rationality of the rapid intensification of Typhoon Haikui determined by CMA using offshore land-based observation data in Qian et al. [22]. In this study, we analyzed the cause, mechanism, and structural changes associated with the rapid intensification of Typhoon Haikui as it moved toward the land.

2 DATA AND MODEL INTRODUCTION

2.1 *Data*

Every year, CMA reports the intensity and position of TC generated in the Northwest Pacific from the operational points at 02:00, 05:00, 8:00, 11:00, 14:00, 17:00, 20:00, and 23:00. A rapid increase in intensity is defined as [3] the time when the change in sea level minimum pressure in the typhoon center within 6 h is less than −7.78 hPa. According to this criterion, Typhoon Haikui rapidly intensified from 08:00 to 14:00 on August 7. The intensity change within 6 h was 15 hPa.

The 6-h National Centers for Environmental Prediction (NCEP) reanalysis data with 1°×1° horizontal resolution were used to supply the initial fields and time-varying lateral boundary conditions for the model. The rapid intensification process of Typhoon Haikui was simulated and analyzed using the Weather Research and Forecast (WRF) model to further explore the cause and mechanism of rapid intensification of Typhoon Haikui.

2.2 *Model description*

The WRF model is used in this study. The simulations contain two domains (d01 and d02) and adopt two-way nesting with the inner nest automatically following the storm center, and the center of the domain is located at 27.5°N, 122.5°E. The size of d01 is 151×121 grid points with horizontal grid spacing of 30 km, while that of d02 is 241×241 grid points with a 10-km horizontal resolution. The model integrates from 20:00 on August 5 and lasts for 96 h. Additional physical process parameters are shown in Table 1.

3 SIMULATION RESULT ANALYSIS

3.1 *Track and strength*

Figure 1 shows the results of numerical simulations of the intensity and track of Typhoon Haikui. The simulated track of the typhoon is similar to the actual track; there is a difference between the simulated and real tracks only at the end of the model integration (Fig.1a). The simulated intensity change is also in good agreement with the real data, and the continuously intensifying process of Typhoon Haikui was simulated successfully. Especially for the period of rapid intensification of Typhoon Haikui from 08:00 to 14:00 on August 7, a decrease in intensity of 9.2 hPa within 6 h was simulated. On the whole, the simulated time and intensity change amplitude of Typhoon Haikui is basically consistent with the current operation. Therefore, the numerical simulation results accurately

Table 1. Model Configuration.

Region	Grid A	Grid B
Grid number	151×121	241×241
Spacing	30 km	10 km
Time step	60 s	60 s
Integration time	0-60 h	0-60 h
Microphysics scheme	WSM3 simple ice scheme	WSM3 simple ice scheme
Cumulus parameterization scheme	Kain-Fritsch (new Eta) scheme	N/A
Land surface process	Noah	Noah

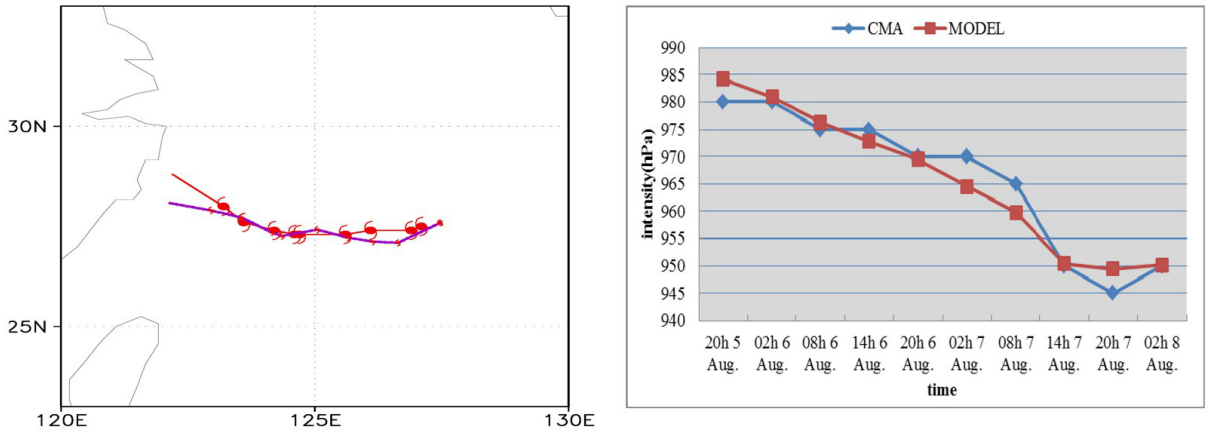

Figure 1. Track (left panel) and intensity (right panel) of Typhoon Haikui determined by the National Meteorological Center of CMA (red line) and by numerical simulation (blue/purple lines).

represent the real track and intensification process of Typhoon Haikui. Now, we focus on analyzing the numerical simulation results to identify the changes of the large-scale background field and mesoscale structural associated with the rapid intensification of Typhoon Haikui.

3.2 *Simulation of land surface pressure field and high–altitude flow field*

Figures 2a and 2c show the 1,000-hPa geopotential height field and 200-hPa high-altitude flow field at 08: 00 and 14:00 on August 7, 2012 just before and after the rapid intensification of Typhoon Haikui. Fig.2 (b and d) shows the numerical simulation results at the same time. Comparing the NCEP reanalysis data with the numerical simulation results for before Typhoon Haikui rapidly intensified (Figs.2a and 2b), we found that the simulated 1,000-hPa geopotential height field and 200-hPa stream field are approximate to the NCEP reanalysis field, and the simulated high-altitude divergence over Typhoon Haikui center and convergence over southeast land in China are also close to the NCEP reanalysis data. In continuous comparison of reanalysis field and numerical results after the rapid intensification of Typhoon Haikui (Figs.2c and 2d), both are approximate including the geopotential height field at 1,000 hPa (in particular, the atmospheric pressure field near the typhoon center) and the intensities and sites of several major weather systems at 200 hPa. Therefore, we may preliminarily argue that the numerical simulation results accurately represent the changes in the environmental field before and after the intensification of Typhoon Haikui.

4 INFLUENCE OF LARGE –SCALE ENVIRONMENTAL FIELD ON TYPHOON INTENSITY

Favorable high-layer and low-layer convergence and divergence conditions and the transport of moisture to the inside of the typhoon play a critical role in rapid increases in typhoon intensity. The previous analysis demonstrated that the numerical simulation results successfully represent large-scale field changes. We further analyzed the effect of changes in environmental field during the rapid intensification process of Typhoon Haikui using numerical simulation.

4.1 *Moisture transport*

Some studies [23-24] have indicated an obvious relationship between the quick increasing of low-level water vapor transportation and the rapid intensification of Typhoon Damrey. Viewed from the 850-hPa flux field of moisture and wind vector field, Typhoon Haikui was symmetrically distributed in the horizontal direction. The moisture mainly supplied from south (Fig.3a). A transport belt began to transport the southern

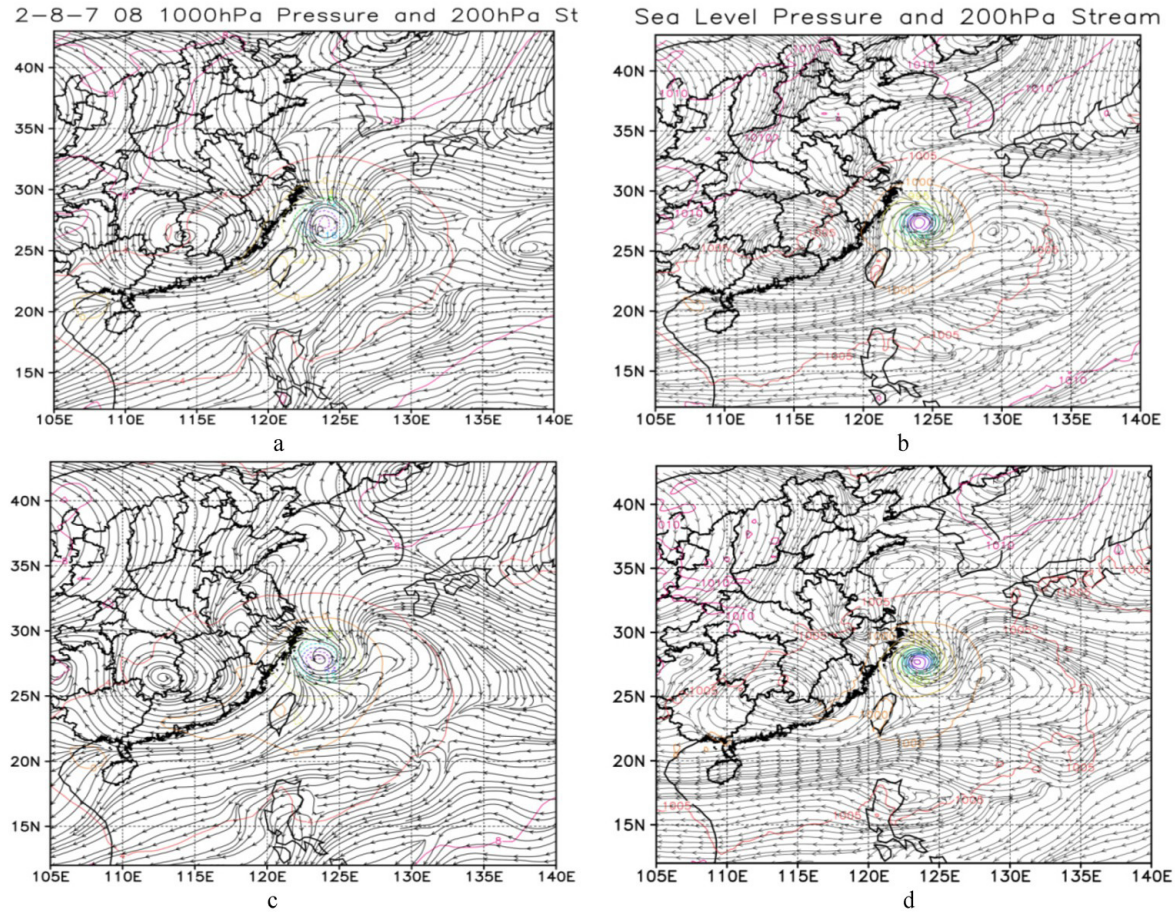

Figure 2. 1,000-hPa geopotential height (contours) and 200-hPa flow field from the NCEP reanalysis data (left panels) and numerical simulation results (right panels) at 08:00 (a and b) and 14:00 (c and d) on August 7, 2012.

moisture to the Haikui environmental flow at 08:00 on August 7 (Fig.3b). The moisture transport channel was completely connected at 14:00 on August 7, and the southern moisture could reach the inside of Typhoon Haikui through the transport belt (Fig.3c). The intensity of moisture transport weakened significantly at 20:00 on August 7 even though the moisture transport channel was connected with the external environmental flow (Fig.d). The moisture transport channel was ruptured at 02:00 on August 8. The amount of transported moisture directly affected the change in the typhoon's strength. The amount of transported moisture increased significantly from 08:00 to 14:00 on August 7, providing the appropriate moisture conditions for the rapid intensification of Typhoon Haikui.

4.2 *Evolution of high-altitude and low-altitude convergence and divergence fields*

While analyzing the change in divergence mean with typhoon movement in 3.5° latitude and longitude grids (equivalent to approximately 400 km) in east, west, south, and north in 850-hPa medium-layer and low-layer and 150-hPa high-layer in Haikui center (Fig.4), we observed that the divergence near the Haikui center was negative in the model integration results, indicating convergence in the low layer and a gradual weakening of convergence intensity. The divergence was positive in the high layer, indicating convergence in this layer and a gradual increase in divergence intensity. The gradual weakening of low-layer convergence intensity did not facilitate the rapid intensification of Typhoon Haikui, whereas the high-layer divergence and low layer convergence in the large-scale background field helped intensify Typhoon Haikui before 20:00 on August 6. From 20:00 on August 6 to 02:00 on August 7, the 850-hPa convergence intensity increased rapidly in the low layer, and the divergence intensity slightly weakened in the high layer. In the following 6 h, the intensity of Typhoon Haikui continued to increase. Notably, from 02:00 to 08:00 on August 7, the convergence in the low layer continued to increase, while the high-layer divergence intensified significantly. Under these large-scale background field configurations, Typhoon Haikui intensified rapidly from 08:00 to 14:00 on August 7, and intensity change in 6 h reached 9.2 hPa. From 08:00 to 14:00 on August 7, the weakening of low-layer convergence was not beneficial to the rapid intensification of the typhoon's intensity, although the high-layer divergence intensity continuously increased. Therefore, the characteristics of time change of high-layer divergence and low-layer difference reflected

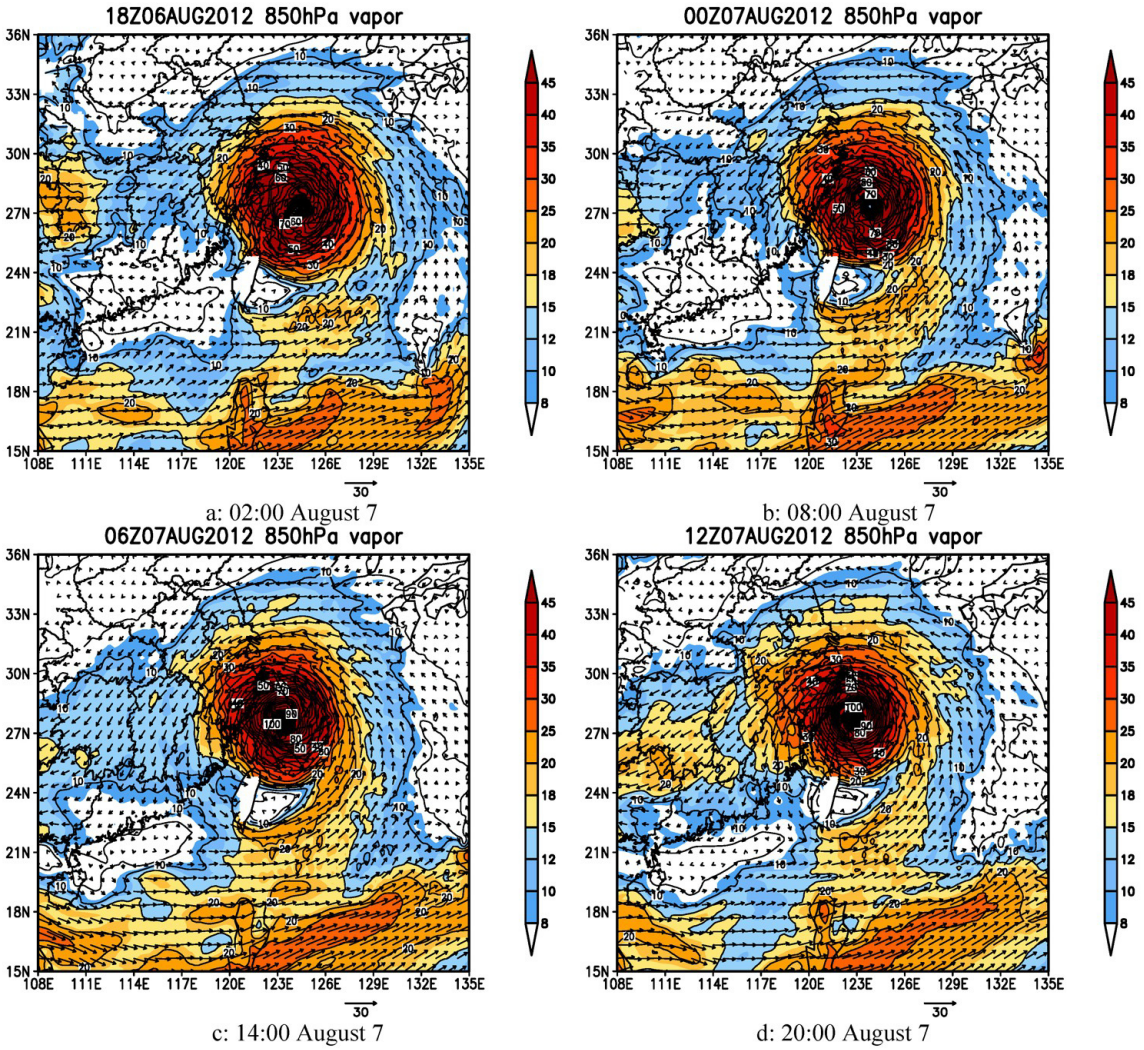

Figure 3. 850-hPa moisture transport flux (contours and shadow distribution in units of $g \cdot cm^{-1} \cdot hPa^{-1} \cdot s^{-1}$) and wind vector time change.

the intensity change of Typhoon Haikui. The simultaneous increase of high-layer divergence and low-layer convergence facilitated the rapid intensification of Typhoon Haikui 6 h ahead.

Further analysis of the vertical divergence profile along the longitude direction across the typhoon center clearly showed the intensification process of high-layer divergence and low-layer convergence near the center of Typhoon Haikui. Notably, the high-layer divergence center moved toward the low layer between 02:00 and 08:00 on August 7, increasing the divergence intensity in the medium layer and high layer across the center of Typhoon Haikui (Figs.5a and b). With the continuous increase in typhoon intensity, the wind field tended to be symmetric, and the high-altitude divergence gradually became more symmetric (Fig.5c). These changes in the large-scale environment field facilitated the intensification of the typhoon intensity.

5 STRUCTURAL EVOLUTION AND ANALYSIS DURING THE RAPID INTENSIFICATION OF TYPHOON HAIKUI

5.1 *Radar echoes*

We analyzed the maximum radar echo output in the model to understand the structural changes during the rapid intensification of Typhoon Haikui. The maximum echo was 50 dBZ just before 14:00 on August 7 (Fig.6a). At 14:00 on August 7, the maximum echo was 55 dBZ (Fig.6d). The echo shape shows that the external southwest spiral echoes gradually evolved from a clustered messy shape to two echo belts. The range of the closed cloud area was slightly smaller at 08:00 on August 7 than that before this time. Afterward, the range of closed cloud area expanded gradually, and two external spiral cloud belts at 10:00 and 12:00 on August 7 evolved into one belt (Figs.6b and c). At 14:

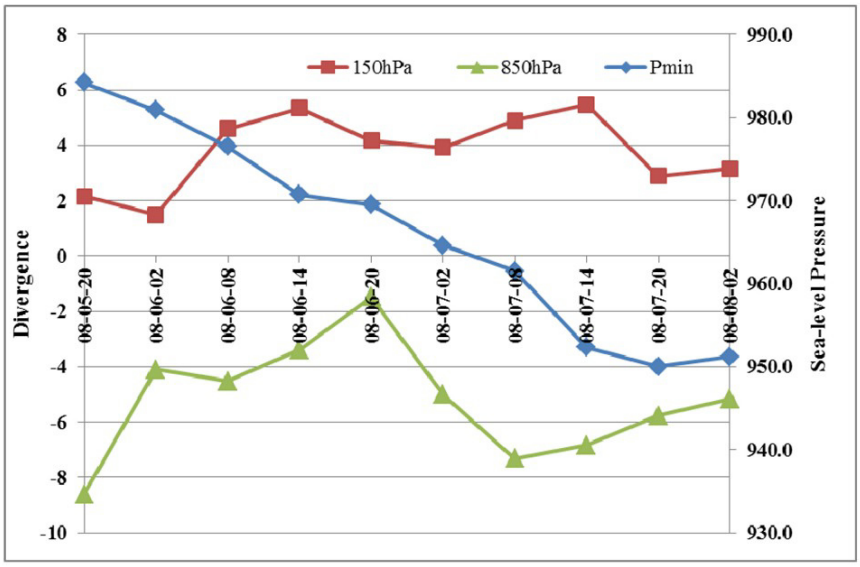

Figure 4. Time dynamic sequence of 150-hPa and 850-hPa divergence field above Typhoon Haikui (in units of 10^{-5} s^{-1}) and simulated intensity (from 20:00 August 5 to 02:00 August 8).

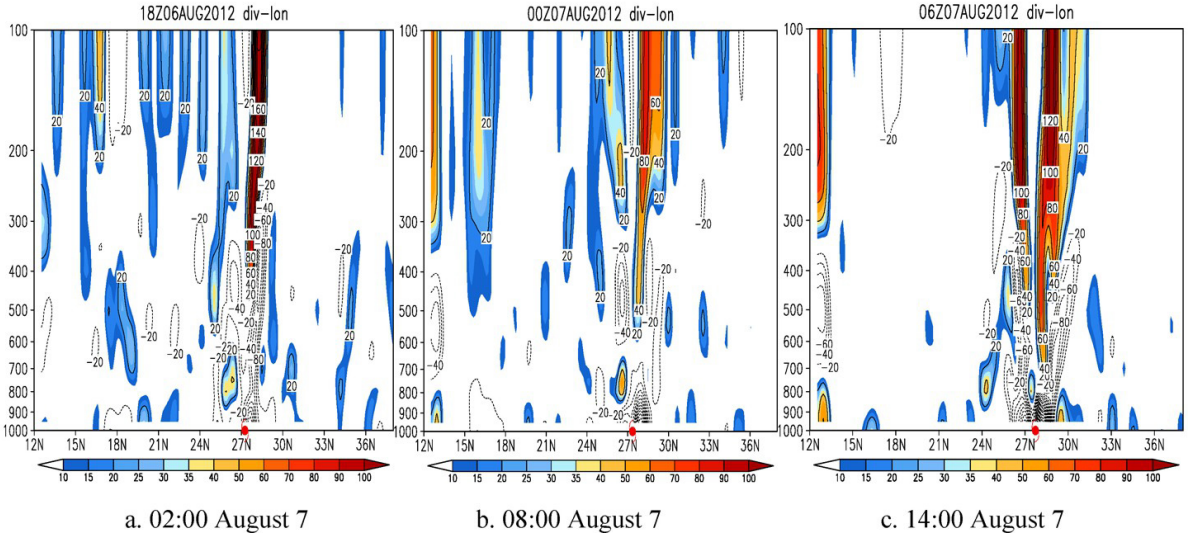

a. 02:00 August 7 b. 08:00 August 7 c. 14:00 August 7

Figure 5. Longitudinal vertical divergence profiles across the center of Typhoon Haikui at different times. Units: 10^{-5} s^{-1}.

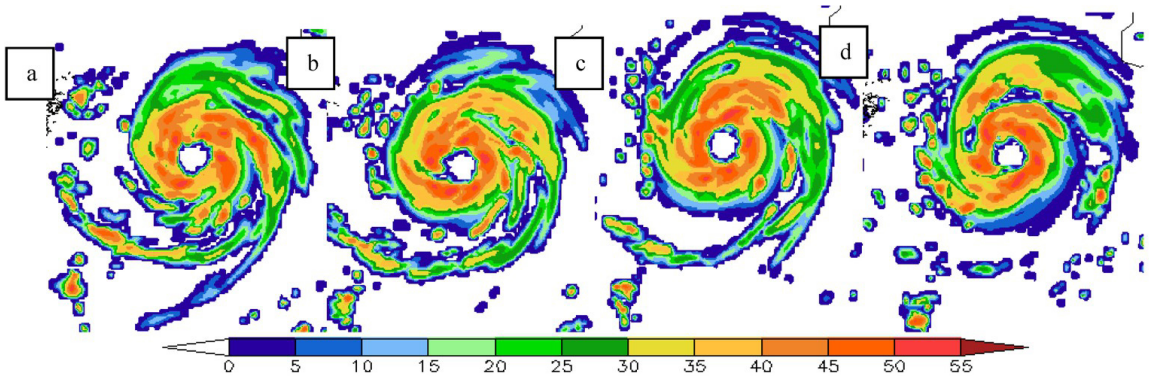

Figure 6. Maximum radar echoes output by model at different times on August 7, 2012: (a) 08:00, (b) 10:00, (c) 12:00, and (d) 14:00. Units: dBZ.

00 on August 7, the southern spiral cloud belt disappeared and became a fragmented echo. The typhoon eye did not change significantly in size, and its diameter was about 80 km. The cloud wall of the typhoon eye changed from slightly loose to compact, suggesting a significant increase in typhoon intensity.

Compared with the evolution of black body temperature from the Japanese Geostationary Meteorological Satellite (Fig.7), the cloud top temperature changed from incompact to compact, while the outer spiral rain band gradually weakened. Thus, the radar echo and cloud top temperature exhibited the same changes.

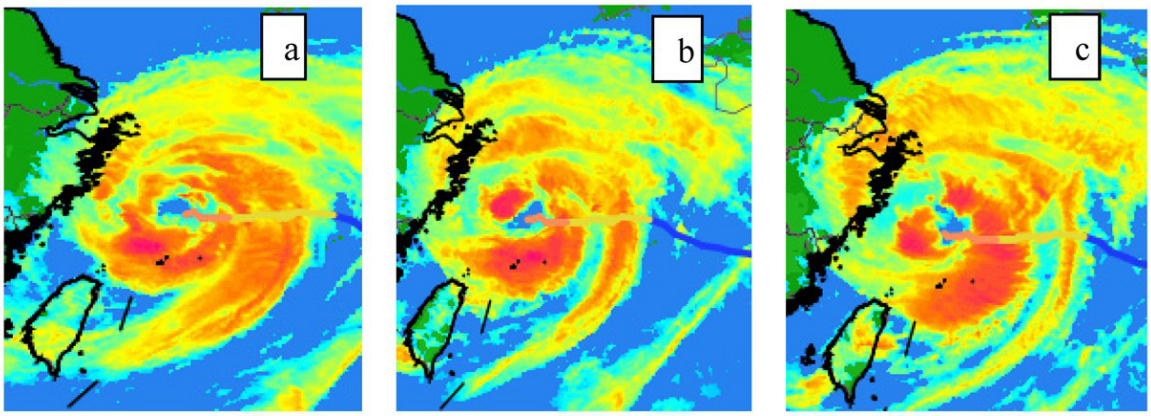

Figure 7. Black body temperature from the Japanese Geostationary Meteorological Satellite at different times on August 7, 2012: (a) 08:00, (b) 10:00, and (c) 12:00.

5.2 *Process of vertical movement symmetry*

The changes in the vertical upward movement in the high layer and low layers were further analyzed. Fig. 8 shows the structural change of vertical movement before and after the rapid intensity change of Typhoon Haikui. Before the rapid intensification of Typhoon Haikui, there was a strong mesoscale convective activity at 850 hPa with sparse distribution, and a strong vertical motion was primarily located on the eastern quadrant. Then the strong mesoscale convective activity was gradually and evenly distributed with the rapid intensification of Typhoon Haikui at 850 hPa at 14:00 on August 7 (Fig.8a). The change in vertical movement on the 300-hPa isobaric surface in the high layer clearly showed that the strong vertical upward movement was primarily focused on the eastern quadrant before the rapid intensification of Typhoon Haikui (Fig.8c). With the increase in typhoon intensity, the strong convective center was evenly distributed in four quadrants close to the typhoon center (Fig.8d). Consequently, the strong convective movement center near the typhoon center changed from an uneven distribution to an even distribution with the rapid typhoon intensification.

5.3 *Radial and tangential winds*

Figure 9 shows the evolution of azimuthally averaged radial and tangential winds based on the model output at the bottom layer (about 32 m from the surface). The wind velocity increased during the period of model integration after 20:00 on August 7, suggesting that the typhoon intensified continuously. In particular, after 02:00 on August 7, the velocities of the radial and tangential winds increased rapidly. The tangential wind intensified from 28 ms^{-1} to 31 ms^{-1} during the typhoon's rapid intensification period (from 08:00 to 14:00 on August 7) and then to 33 ms^{-1} at 20:00 on August 7. The absolute value of radial wind velocity increased to 14 ms^{-1} at 14:00 on August 7 and rapidly to 18 ms^{-1} in the subsequent 6 h, suggesting that TC inflow increased, and that the intensified convergence aided the increase in typhoon intensity. Moreover, the radius of maximum wind (RMW) reduced significantly from 90 km to about 60 km, and the shrinkage of the cloud wall of the typhoon eye finished before and after the time of rapid intensification of Typhoon Haikui, which agreed with the simulation results reported by Liu et al.[25] and Deng et al. [26], possibly because of the angular momentum conservation with increased TC intensity and radial and tangential winds.

Figure 10 shows the vertical evolution of radial and tangential winds. The maximum tangential wind has a velocity greater than 35 ms^{-1} was found 1–2 km from the land surface at 20:00 on August 6 (Fig.10a). The maximum tangential wind with velocity greater than 35 ms^{-1} gradually developed toward a higher altitude of over 7 km at 08:00 on August 7. The wind velocity over 7 km decreased gradually, and RMW axle inclined outwardly (Fig.10b). This structure is characteristic of a typical mature typhoon inner core [27]. At 14:00 on August 7, the height of the maximum wind velocity was approximately 10 km (Fig.10c). From 08:00 to 14:00 on August 7, the range of maximum wind velocity expanded significantly, and the radius of the wind with

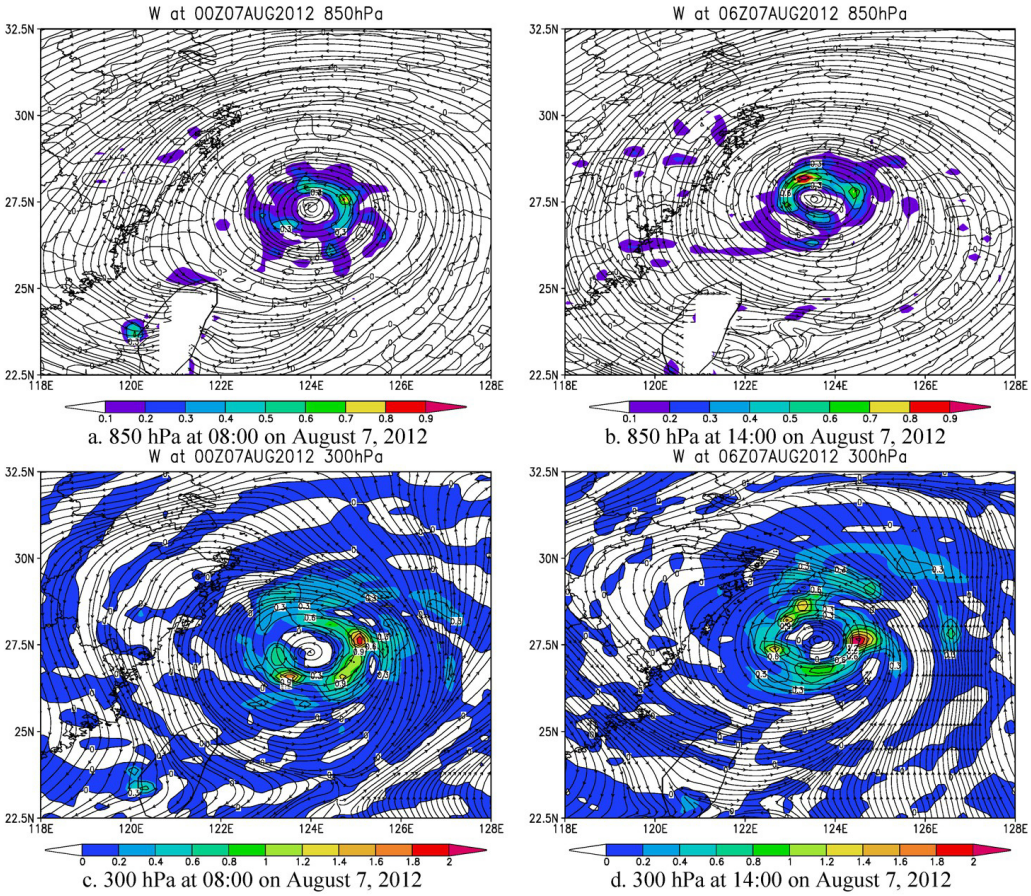

Figure 8. Changes in high-layer and low-layer vertical velocity and flow field during the rapid intensification of Typhoon Haikui. Units: ms^{-1}.

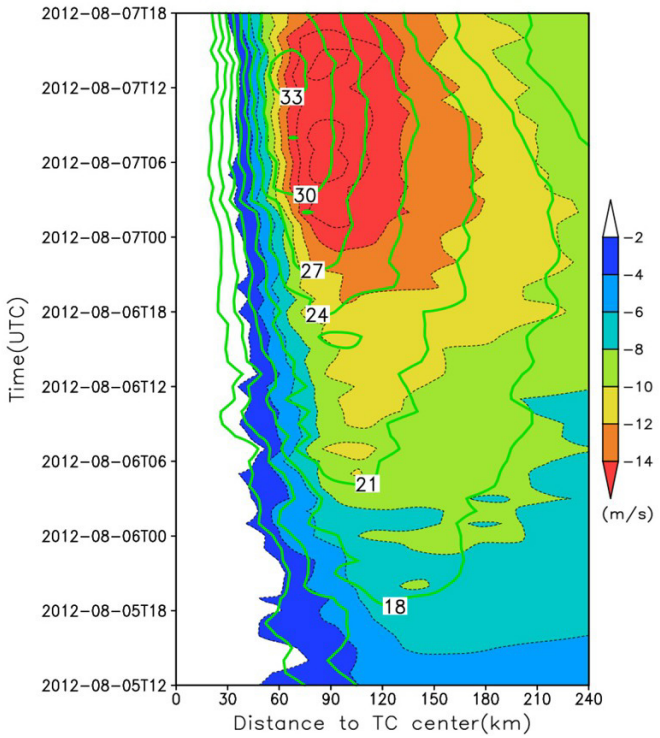

Figure 9. Evolution of azimuthally averaged radial wind (colored block) and tangential wind (contour) based on the model output at the bottom layer (in units of ms^{-1}) (left ordinate is for coordinated universal time).

velocity greater than 35 ms^{-1} was within 60–140 km around from the typhoon center. Afterward, the height and range were reduced slightly. The analysis of the vertical profile of tangential wind velocity showed that the typhoon intensity increased significantly from 08:00 to 14:00 on August 7.

Based on the radial wind velocity, the main inflow was located beneath 1 km and extended 240 km outside of the center of the typhoon in the horizontal direction and rapidly attenuated 40 km from the typhoon center. The inflow intensity reached 12 ms^{-1}, and the inflow in the typhoon eye area (within 40 km of the eye) was weak (less than 1 ms^{-1}). The main outflow was located at a height of approximately14 km and reached 9 ms^{-1} commonly and 12 ms^{-1} maximally. During the rapid intensification period (from 08:00 to 14:00 on August 7; Figs. 10b and c), a 9 ms^{-1} positive value occurred at a height of 2–4 km, 60 km from the typhoon center. This suggested the significant increase in low-layer outflow. Furthermore, the outflow axle inclined outward with height. All these reflected that the high-layer and low-layer of TC helped secondary environmental flow for intensity development, especially at rapid intensifying time.

According to the evolution of the vertical cross-section of radial velocity in Fig.10, inflow was all beneath 1 km, while the inflow intensified with the decreasing altitude, suggesting that the frictional effect of the ocean surface was not significant. Inflow 240 km away from the typhoon center intensified continuously and reached a maximum at 100 km away from the center of the typhoon, and then weakened. A faint outflow remained within 40 km from the typhoon center. The maximum outflow occurred at a height of 13–16 km at 08:00 on August 7, and then declined to 11–15 km, while the wind velocity exceeded 10 ms^{-1} at this height. Between 2 km and the height of maximum outflow, the strong outflow remained with increasing altitude between 40 km and 100 km apart from the TC center, which occurred at 08:00 on August 7 and then intensified to some extent. The involution suggested that the structural changes facilitated the intensification of Typhoon Haikui during this period.

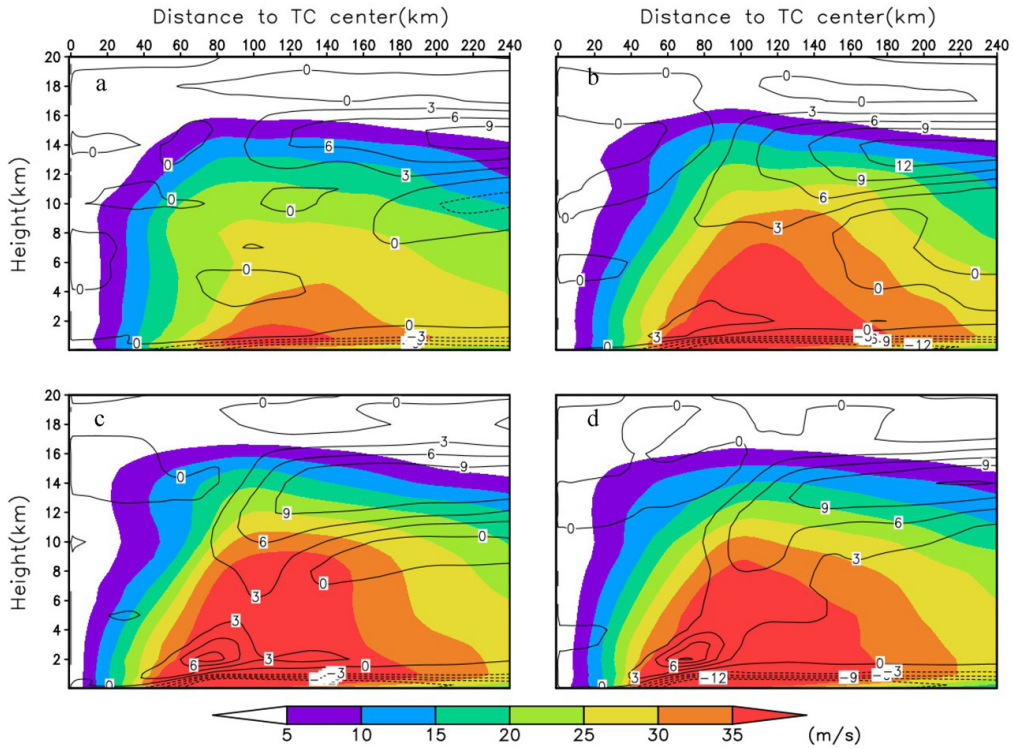

Figure 10. Vertical cross-section of radial wind (contour) and tangential wind (colored block) at different times: (a) 20:00 August 6, (b) 08:00 August 7, (c) 14:00 August 7, and (c) 20:00 August 7 (in unit of ms^{-1}).

5.4 *Atmospheric temperature anomaly and vertical velocity*

The shaded area in Fig.11 shows the distribution of temperature anomaly. The warm core was near the typhoon center at an altitude of 8–12 km and gradually extended outward, especially from 08:00 to 14:00 on August 7, 2012. Furthermore, the warm core intensified with increasing typhoon intensity. During this time, the temperature anomaly changed from 7 ℃ on August 6 to 11 ℃ on August 7. At altitudes above 16 km, the warm core intensity decreased gradually with altitude until the temperature anomaly became negative, which indicated the height at which the ascending motion near the typhoon center could arrive. With the increasing

intensity of Typhoon Haikui, the warm core expanded toward the lower level. The 8 ℃ temperature anomaly contour at 02:00 on August 7 was at an altitude of 10 km, and then expanded downward to altitudes of 8 km at 08:00 on August 7 and 6 km on August 8, 2012. The analyses of the distribution of temperature anomaly near the typhoon center conclusively showed that typhoon intensity increased during this period.

From the evolution of the cross-section of vertical velocity in Fig. 11 we can see that the vertical velocity was generally small before August 7. A large updraft velocity occurred after 08:00 on August 7. The maximum updraft velocity was 1.2 ms^{-1} at about 90 km from the center of the typhoon and at altitudes of about 6 km, and the width of a large updraft belt was about 20–30 km.

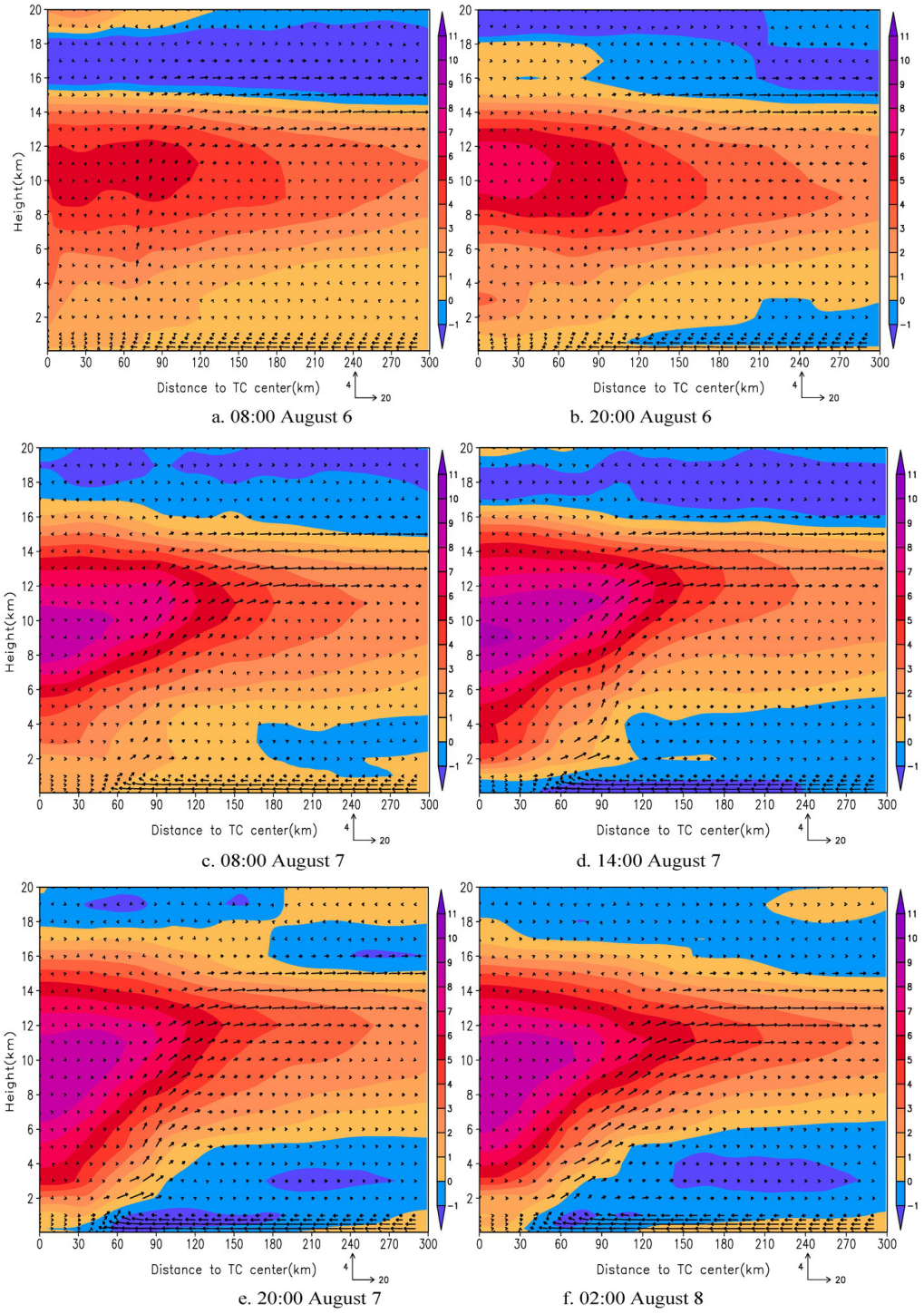

Figure 11. The vertical cross-section of atmospheric temperature anomaly (shaded; units of ℃) and the combination of tangential wind and vertical velocity (in 1:5; units of ms^{-1}).

6 CONCLUSION

Numerical simulation was performed for Typhoon Haikui before and after the rapid offshore intensification using mesoscale WRF (V3.3). The model best simulated the offshore intensification and rapid offshore intensification. Diagnostic analysis was then preformed on the simulation output to draw conclusions as follows:

(1) The rapid intensification of Typhoon Haikui was substantially correlated with the significant low-layer moisture input and the increased low-layer convergence and high-layer divergence. The intensification of low-level convergence and high-level divergence occurred about 6 h before the rapid intensification of Typhoon Haikui. During the period of the rapid intensification of Typhoon Haikui, due to the insignificant frictional effects of the boundary layer when the typhoon moves over the ocean surface, the radial wind increased and the inflow was intensified with the decreasing height beneath 1 km from the sea surface.

(2) During the intensification of Typhoon Haikui, the typhoon structure changed significantly. The structural changes in Typhoon Haikui were a major cause of its rapid intensification. The typhoon structure was very symmetrical, the range of the cloud wall of the typhoon eye was small, and the range of the cloud wall of the typhoon eye in the high layer extended outward. The radial velocity and tangential velocity increased, particularly during the period of rapid typhoon intensification. The warm core gradually intensified from August 6 to 7, and the temperature anomaly near the typhoon center increased from 6−7℃ to 11℃. The warm core of the typhoon was mainly at a height of 8−12 km from the land surface, and the range of the warm core extended outward and considerably toward the lower layer during the intensification process. A strong updraft velocity appeared after 08:00 on August 7 and reached a maximal intensity between 14:00 and 20:00 on August 7. The updraft velocity at maximum intensity was 1.2 ms^{-1} and occurred at about 90 km from the typhoon center at an altitude of about 6 km. These structural changes in the typhoon facilitated its rapid intensification.

REFERENCES:

[1] CHEN Lian-shou, DING Yi-hui. The Perspective of Typhoon in the Western Pacific [M]. Beijing: Science Press, 1979, 491pp.

[2] YAN Jun-yue. Climatological Characteristic of rapidly Intensifying Tropical Cyclones over the Offshore of China [J]. Quart J Appl Meteor, 1996, 7(1): 28-35.

[3] YU Yu-bin, YAO Xiu-ping. A Statistical Analysis on Intensity Change of Tropical Cyclone over the Western North Pacific [J]. J Trop Meteor, 2006, 22(6): 521-526.

[4] YU Run-ling, YU Hui, DUAN Yi-hong. A Statistical Analysis on Intensity Change of Tropical Cyclone Prior to landfall [J]. J Trop Meteor, 2011, 27(1): 74-81.

[5] ZHU Xiao-jin, CHEN Lian-shou. Climatological Characteristics of Rapidly Intensifying Tropical Cyclone over the Coastal Waters of China and the Relationship with ENSO [J]. Acta Sci Nat Univ Pekinensis, 2011, 47 (1): 52-58.

[6] HU Shu, LI Ying, XU Ying-long. A Statistical Analysis on Intensity and Structure Change of Tropical Cyclone making Landfall on Taiwan Island [J]. J Trop Meteor, 2012, 28(3): 300-310.

[7] XU Ying-long, ZHANG Ling, GAO Shuan-zhu. The Advances and Discussion on China Operational Typhoon Forecasting [J]. Meteor Mon, 2010, 36(7): 43-49.

[8] CHEN Lian-shou, MENG Zhi-yong. An Overview on Tropical Cyclone Research Progress in China during the Past ten years [J]. Chin J Atmos Sci, 2001, 25(3): 420-432.

[9] DUAN Yi-hong, YU Hui, WU Rong-sheng. Review of the Research in the Intensity Change of Tropical Cyclone [J], Acta Meteor Sinica, 2005, 63(5): 636-645.

[10] YU Hui, FEI Liang, DUAN Yi-hong. Favorable large-scale conditions for rapid intensification of typhoon "Bill" and "Jelawat" before their landfall [J]. Acta Meteor Sinica, 2002, 60 (S1): 78-87.

[11] LIANG Jian-yin, CHEN Zi-tong, WAN Qi-lin et al. Diagnostic Analysis of the Landfall process Tropical Cyclone "Vongfong" [J]. J Trop Meteor, 2003, 19(S1): 45-55.

[12] HU Chun-mei, DUAN Yi-hong, YU Hui, et al. The Diagnostic Analysis of Rapid Change in Tropical Cyclones Intensity before Landfall in South China [J]. J Trop Meteor, 2005, 21(4): 377-382.

[13] CHEN P-Y, YU H, CHAN J C L. Western North Pacific tropical cyclone intensity prediction scheme [J]. Acta Meteor Sinica, 2011, 6(5): 611-624.

[14] LEI Xiao-tu, CHEN Lian-shou. Dynamical Studies on the Effect of Large-scale Environmental Flow on Tropical Cyclones [J]. Acta Meteor Sinica, 2001, 59(4): 429-439.

[15] WANG Yu-qing. Recent research progress on tropical cyclone structure and intensity [J]. Trop Cyclone Res Rev, 2012: 1(2): 254-275.

[16] CHEN Lian-shou, XU Xiang-de, LUO Zhe-xian, et al. Introduction of Tropical Cyclone Dynamics [M]. Beijing: China Meteorological Press, 2002: 317pp.

[17] LUO Zhe-xian. Nonlinear Interaction of Axisymmetric Circulation and Non-axisymmetric disturbances in hurricanes [J]. Sci China (Ser D), 2004, 47, 58-67.

[18] LI Ying, CHEN Lian-shou, WANG Ji-zhi. The Diagnostic Analysis of Characteristics of Large Scale Circulation Corresponding to the Sustaining and Decaying of Tropical Cyclone after its Landfall [J]. Acta Meteor Sinica, 2004, 62(2): 167-179.

[19] LI Ying, CHEN Lian-shou, WANG Ji-zhi. Diagnostic Study of the Sustaining and Decaying of Tropical Cyclones after Landfall [J]. Chin J Atmos Sci, 2005, 29 (3): 482-490.

[20] YU Yu-bin, CHEN Lian-shou, YANG Chang-xian. The features and mechanism analysis on rapid intensity change of super typhoon Saomai (2006) over the offshore of China [J]. Chin J Atmos Sci, 2008, 32(2): 405-416.

[21] ZENG Zhi-hua, CHEN Lian-shou, WANG Yu-qing, et al. A numerical simulation study of super Typhoon Saomei (2006) intensity and structure changes [J]. Acta Meteor Sinica, 2009, 67(5): 750-763.

[22] QIAN Yan-zhen, GAO Shuan-zhu, HUANG Si-yuan, et al. Analysis on intensity variation of Haikui before and after its landing [J]. Meteor Mon, 2013, 39 (10): 1265-1274.

[23] GUAN Xiao-jun. Numerical simulation of rapid intensity change of Typhoon Damrey [J]. Meteor Sci Tech, 2012, 40(2): 241-248.

[24] DONG Liang-miao, CHEN Jian, HE Dong-yan. An analysis of the cause of the intensity change of the "0518" TY Damey in its late phase [J]. Marine Forecasts, 2008, 25(3): 28-32.

[25] DENG Guo, ZHOU Yu-shu, YU Zhan-jiang. Analysis of water vapor transportation in Typhoon Dan (9914) [J]. J Trop Meteor, 2005, 21(5): 533-541.

[26] LIU Y-B, ZHANG D-L, YAU M K. A multiscale numerical study of Hurricane Andrew (1992) Part II: Kinematics and inner-core structure [J]. Mon Wea Rev, 1998, 127(911): 2597-2616.

[27] XU Xiang-chun, YU Yu-bin, WANG Shi-gong, et al. Simulation on evolution of the inner-core structure of Typhoon Damrey over Hainan Island [J]. J Trop Oceanogr, 2012, 31(4): 66-74.

Citation: ZHANG Sheng-jun, QIAN Yan-zhen, HUANG Yi-wu et al. Numerical simulation study on the rapid intensification of typhoon Haikui (1211) off the shore of China [J]. J Trop Meteor, 2017, 23(3): 269-280.